Hidden Charm Pentaquarks
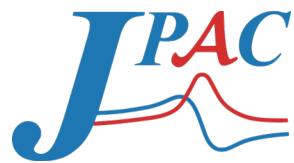
M. en C. Jorge Antonio Silva-Castro

Universidad Nacional Autónoma de México

Exotic heavy meson spectroscopy and structure with EIC (2022)

The Pc(4312)
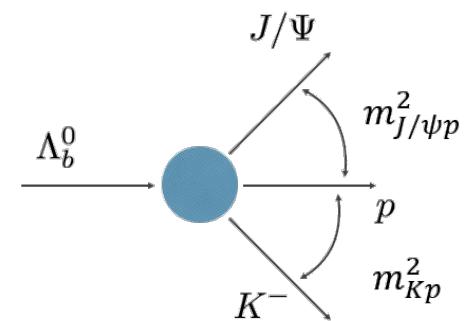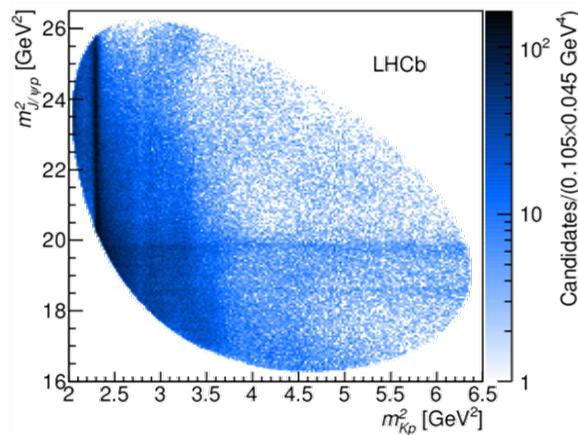
In our analysis we focus on the narrow signal named Pc(4312) which is 5MeV below the $\Sigma_C^+ \overline{D}^0$ threshold.

The Pc(4312)

In our analysis we focus on the narrow signal named Pc(4312) which is 5MeV below the $\Sigma_C^+ \overline{D}^0$ threshold.

LHCb, PRL 122 (2019) 222001

The Pc(4312)

In our analysis we focus on the narrow signal named Pc(4312) which is 5MeV below the $\Sigma_C^+ \overline{D}^0$ threshold.

LHCb, PRL 122 (2019) 222001

The Pc(4312)

In our analysis we focus on the narrow signal named Pc(4312) which is 5MeV below the $\Sigma_c^+ \overline{D}^0$ threshold.

Pc(4312)

$\Sigma_c^+ \overline{D}^0$ th.

Data: LHCb
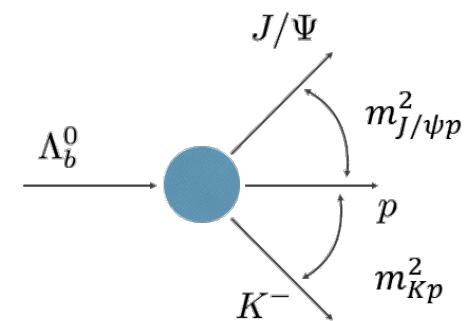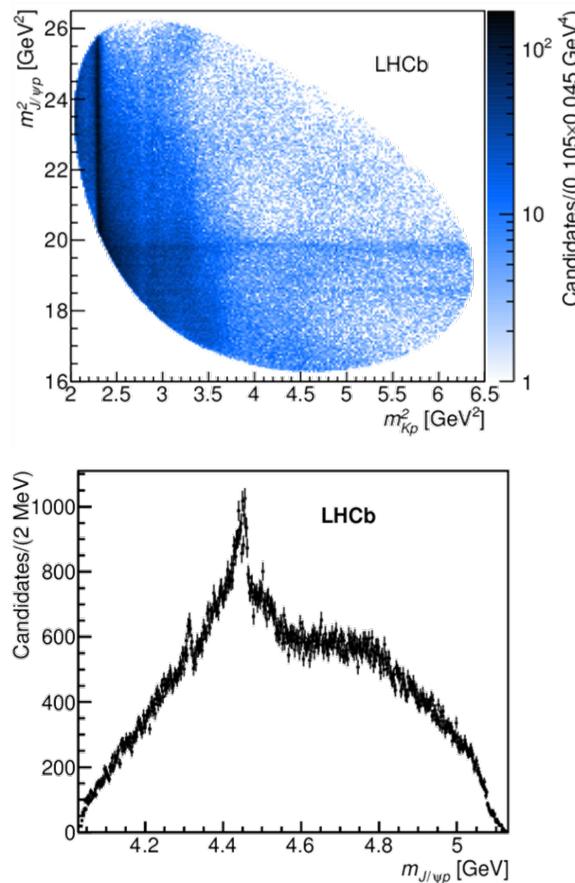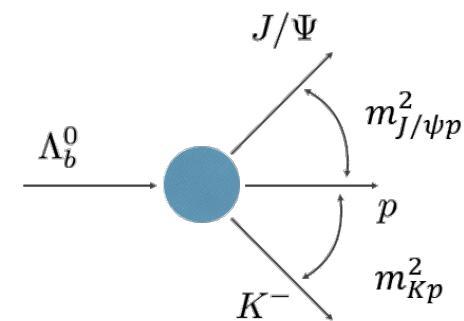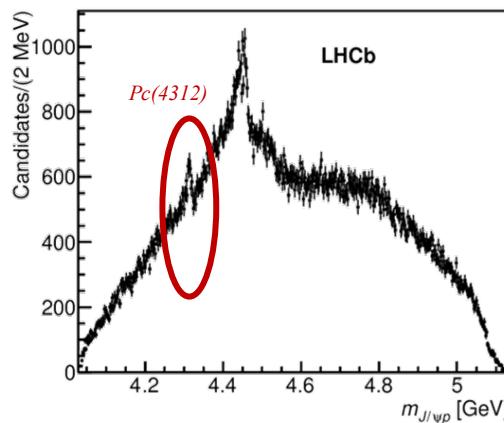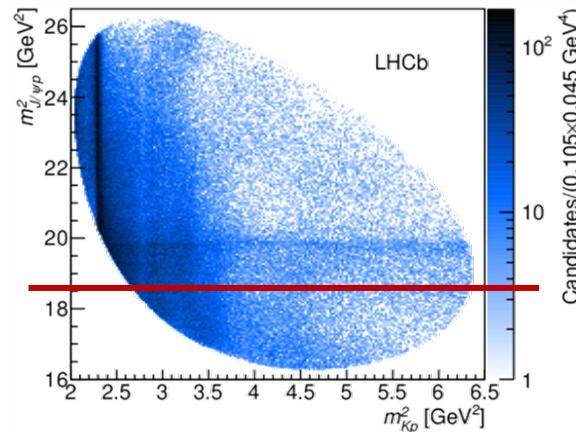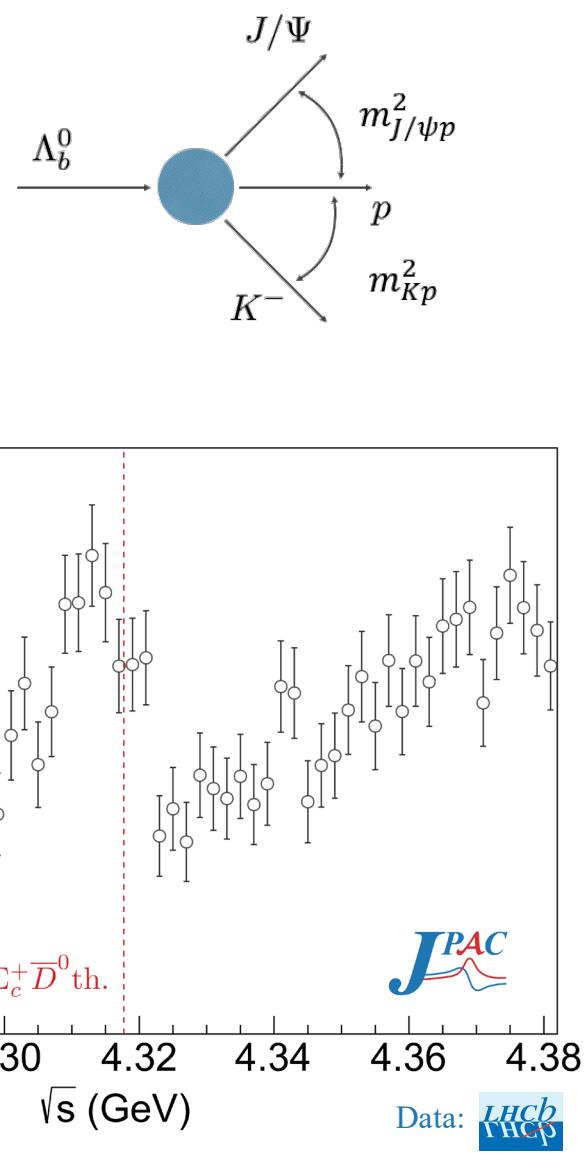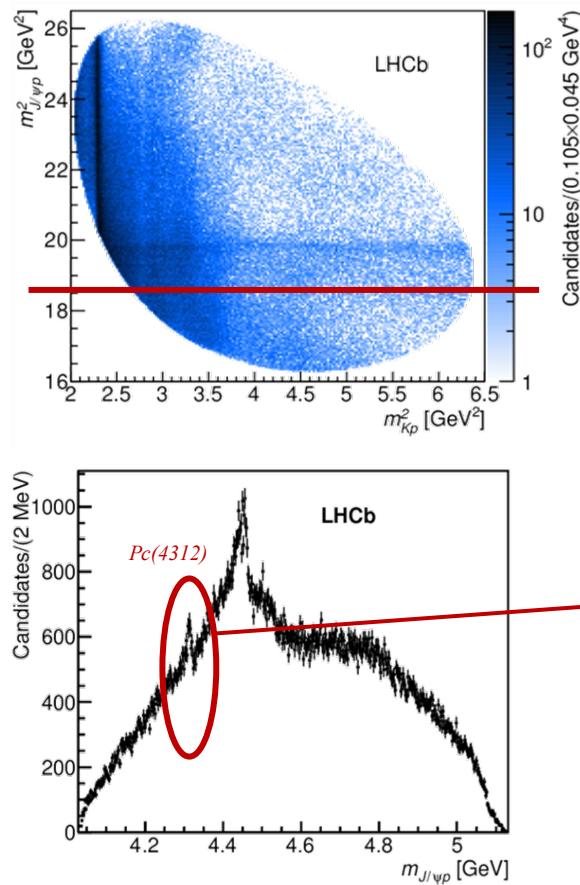
LHCb, PRL 122 (2019) 222001

Possible interpretations

The various interpretations of the signal are related to different analytic properties of the amplitude:
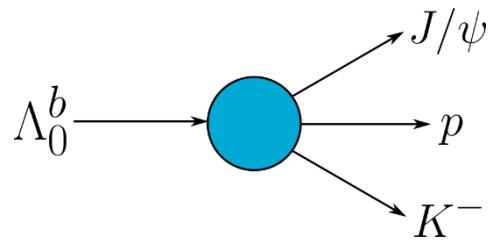
studied in LHCb 1904.03947
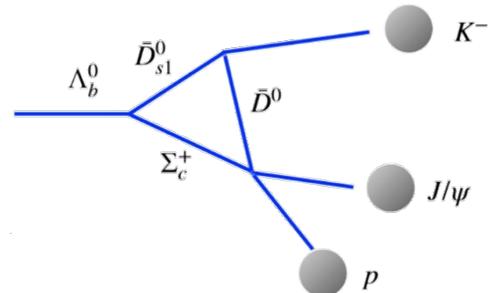
Ali, Parkhomenko 1904.00446
Holma, Ohlsson 1906.08499
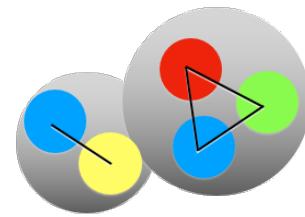
Wu et al. 1007.0573
Liu et al. 1903.11560
Du et al. 1910.11846
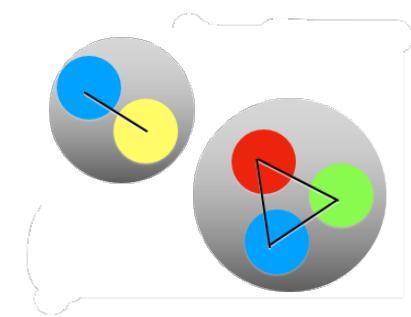
Burns, Swanson 1908.03528
Fernández-Ramírez et al. 1904.10021

Near threshold theory: hypotheses

- Only one partial wave contributes to the Pc signal

- The threshold drives the physics

- Further singularities are irrelevant

Near threshold theory: hypotheses

- Only one partial wave contributes to the Pc signal

- The threshold drives the physics

- Further singularities are irrelevant

We have no information about the quantum numbers of the signal

Near threshold theory: hypotheses

- Only one partial wave contributes to the Pc signal

- The threshold drives the physics

- Further singularities are irrelevant

We have no information about the quantum numbers of the signal

We construct a reaction amplitude that respects the generic principles of the S-matrix theory, and fit directly the experimental $J/\psi\, p$ mass distribution, considering the experimental resolution.

The complete S-matrix has undetermined parameters which encode the underlying QCD dynamics. We leave them to be determined by data, rather than by a given model.

Near threshold theory: equations

Event distribution in 4250-4380 MeV range:

$$\frac{dN}{d\sqrt{s}} = \rho(s)[|F(s)|^2 + B(s)]$$

Phase space factor

Pc signal + coherent bkg

Incoherent bkg

Frazer, Hendry, PR 134 (1964) B1307

Near threshold theory: equations

Event distribution in 4250-4380 MeV range:

$$\frac{dN}{d\sqrt{s}} = \rho(s)[|F(s)|^2 + B(s)]$$

Phase space factor

Incoherent bkg

Pc signal + coherent bkg

$$F(s) = \quad P_i \quad T_{ij}$$

Λ_b^0 J/ψ

K^+ p

$J/\psi\, p \to J/\psi\, p$

Frazer, Hendry, PR 134 (1964) B1307

Near threshold theory: equations

Event distribution in 4250-4380 MeV range:

$$\frac{dN}{d\sqrt{s}} = \rho(s)[|F(s)|^2 + B(s)]$$

Phase space factor

Pc signal + coherent bkg

Incoherent bkg

$$F(s) = \quad$$

$$J/\psi\, p \rightarrow J/\psi\, p$$

Coupled channel amplitude:

Channel 1: $J/\psi p$

Channel 2: $\Sigma_c^+ \overline{D}^0$

$$\left(T^{-1}\right)_{ij} = M_{ij} - i k_i \delta_{ij}$$

Four Riemann sheets

$$k_i = \sqrt{s - s_i} \qquad s_1 = \left(m_\psi + m_p\right)^2 \qquad s_2 = \left(m_{\Sigma_c^+} + m_{\overline{D}^0}\right)^2$$

Near threshold theory: equations

Event distribution in 4250-4380 MeV range:

$$\frac{dN}{d\sqrt{s}} = \rho(s)[|F(s)|^2 + B(s)]$$

Phase space factor

Incoherent bkg

Pc signal + coherent bkg

$F(s) =$ Λ_b^0 K^+ P_i T_{ij} J/ψ p

$J/\psi\, p \to J/\psi\, p$

Coupled channel amplitude:

Channel 1: $J/\psi p$

Channel 2: $\Sigma_c^+ \overline{D}^0$

$$\left(T^{-1}\right)_{ij} = M_{ij} - i k_i \delta_{ij}$$

Four Riemann sheets

$$k_i = \sqrt{s - s_i} \qquad s_1 = \left(m_\psi + m_p\right)^2 \qquad s_2 = \left(m_{\Sigma_c^+} + m_{\overline{D}^0}\right)^2$$

M_{ij} are singularity free and can be Taylor expanded

$$M_{ij}(s) = m_{ij} - c_{ij}s + \cdots$$

Near threshold theory: equations

Event distribution in 4250-4380 MeV range:

$$\frac{dN}{d\sqrt{s}} = \rho(s)[|F(s)|^2 + B(s)]$$

Phase space factor

Pc signal + coherent bkg

Incoherent bkg

$$F(s) = $$

$$J/\psi\, p \to J/\psi\, p$$

Coupled channel amplitude:

Channel 1: $J/\psi p$

Channel 2: $\Sigma_c^+ \overline{D}^0$

$$\left(T^{-1}\right)_{ij} = M_{ij} - ik_i\delta_{ij}$$

Four Riemann sheets

$$k_i = \sqrt{s - s_i} \qquad s_1 = \left(m_\psi + m_p\right)^2 \qquad s_2 = \left(m_{\Sigma_c^+} + m_{\overline{D}^0}\right)^2$$

M_{ij} are singularity free and can be Taylor expanded

$$M_{ij}(s) = m_{ij} - c_{ij}s + \cdots$$

Scattering length

Frazer, Hendry, PR 134 (1964) B1307

Near threshold theory: equations

Event distribution in 4250-4380 MeV range:

$$\frac{dN}{d\sqrt{s}} = \rho(s)[|F(s)|^2 + B(s)]$$

Phase space factor (points to $\rho(s)$)

Pc signal + coherent bkg (points to $|F(s)|^2$)

Incoherent bkg (points to $B(s)$)

$$F(s) = \boxed{P_i} - \boxed{T_{ij}}$$

(diagram: Λ_b^0, K^+ entering P_i; J/ψ, p exiting T_{ij})

$J/\psi\, p \to J/\psi\, p$

Coupled channel amplitude:

Channel 1: $J/\psi p$

Channel 2: $\Sigma_c^+ \overline{D}^0$

$$\left(T^{-1}\right)_{ij} = M_{ij} - i k_i \delta_{ij}$$

Four Riemann sheets

$$k_i = \sqrt{s - s_i} \qquad s_1 = \left(m_\psi + m_p\right)^2 \qquad s_2 = \left(m_{\Sigma_c^+} + m_{\overline{D}^0}\right)^2$$

M_{ij} are singularity free and can be Taylor expanded $\qquad M_{ij}(s) = m_{ij} - c_{ij}s + \cdots$

Scattering length (brace under c_{ij})

Effective range (brace under $c_{ij}s$)

Frazer, Hendry, PR 134 (1964) B1307

Near threshold theory: equations

The functions $B(s)$, P_1 and T_{11} are then:

$$B(s) = b_0 + b_1 s$$

$$F(s) = (p_0 + p_1 s) \frac{[m_{22} - c_{22}s - ik_2]}{[m_{22} - c_{22}s - ik_2][m_{11} - c_{11}s - ik_1] - m_{12}^2}$$

Frazer, Hendry, PR 134 (1964) B1307

Near threshold theory: equations

The functions $B(s)$, P_1 and T_{11} are then:

$$B(s) = b_0 + b_1 s$$

Channel coupling

$$F(s) = (p_0 + p_1 s) \frac{[m_{22} - c_{22}s - ik_2]}{[m_{22} - c_{22}s - ik_2][m_{11} - c_{11}s - ik_1] - m_{12}^2}$$

Background, production, hyperons and effects due to further singularities.

Frazer, Hendry, PR 134 (1964) B1307

Near threshold theory: equations

The functions $B(s)$, P_1 and T_{11} are then:

Channel coupling

$$B(s) = b_0 + b_1 s$$

$$F(s) = (p_0 + p_1 s) \frac{[m_{22} - c_{22}s - ik_2]}{[m_{22} - c_{22}s - ik_2][m_{11} - c_{11}s - ik_1] - m_{12}^2}$$

Background, production, hyperons and effects due to further singularities.

The case $c_{ii} = 0$ corresponds to the *scattering length*, and when $c_{ii} \neq 0$ corresponds to the *effective range*.

Frazer, Hendry, PR 134 (1964) B1307

Near threshold theory: equations

The functions $B(s)$, P_1 and T_{11} are then:

$$B(s) = b_0 + b_1 s$$

Channel coupling

$$F(s) = (p_0 + p_1 s) \frac{[m_{22} - c_{22}s - ik_2]}{[m_{22} - c_{22}s - ik_2][m_{11} - c_{11}s - ik_1] - m_{12}^2}$$

Background, production, hyperons and effects due to further singularities.

The case $c_{ii} = 0$ corresponds to the *scattering length*, and when $c_{ii} \neq 0$ corresponds to the *effective range*.

If $c_{ii} = 0$ poles can appear onto the second or fourth Riemann sheet.

The $c_{ii} \neq 0$ are corrections that appears as we move away from the threshold with poles in any Riemann sheet.

*Frazer, Hendry, PR 134 (1964) B1307*

Fit and error analysis

To fit the data and to estimate the sensitivity of the pole positions to the uncertainties, we use the bootstrap technique with 10^4 pseudodata sets.
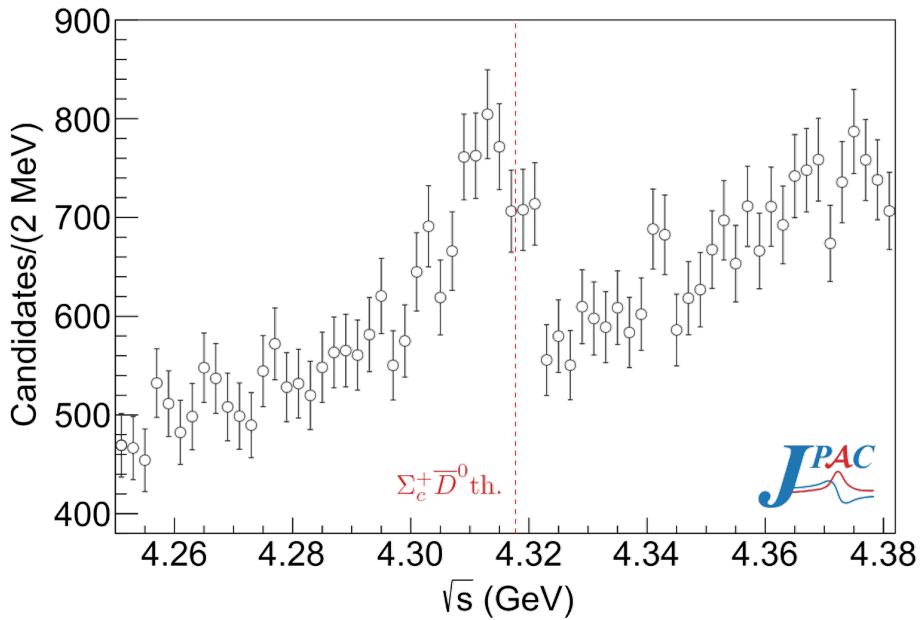
Fit and error analysis

To fit the data and to estimate the sensitivity of the pole positions to the uncertainties, we use the bootstrap technique with 10^4 pseudodata sets.
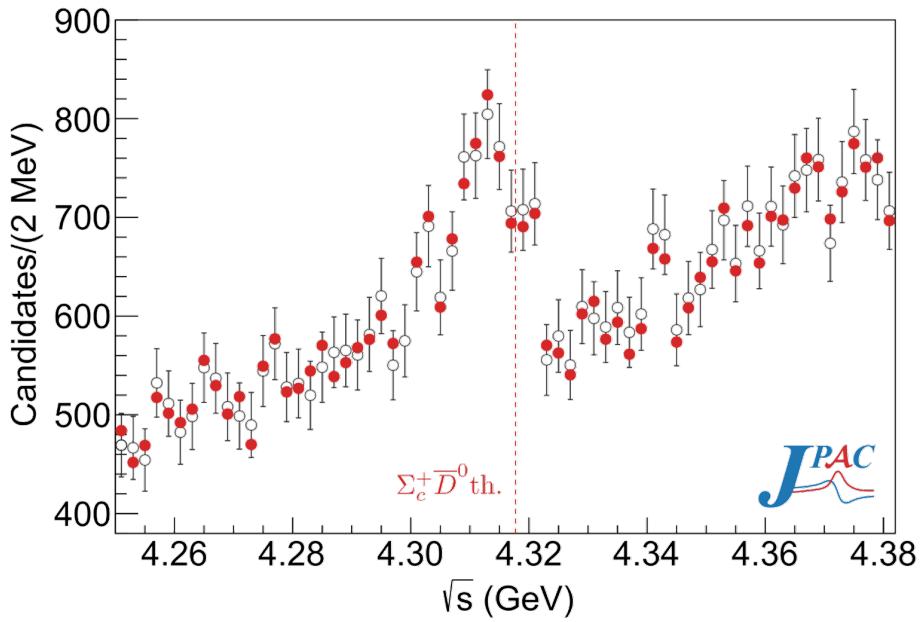
We generate compatible pseudodata from LHCb data.

Fit and error analysis

To fit the data and to estimate the sensitivity of the pole positions to the uncertainties, we use the bootstrap technique with 10^4 pseudodata sets.
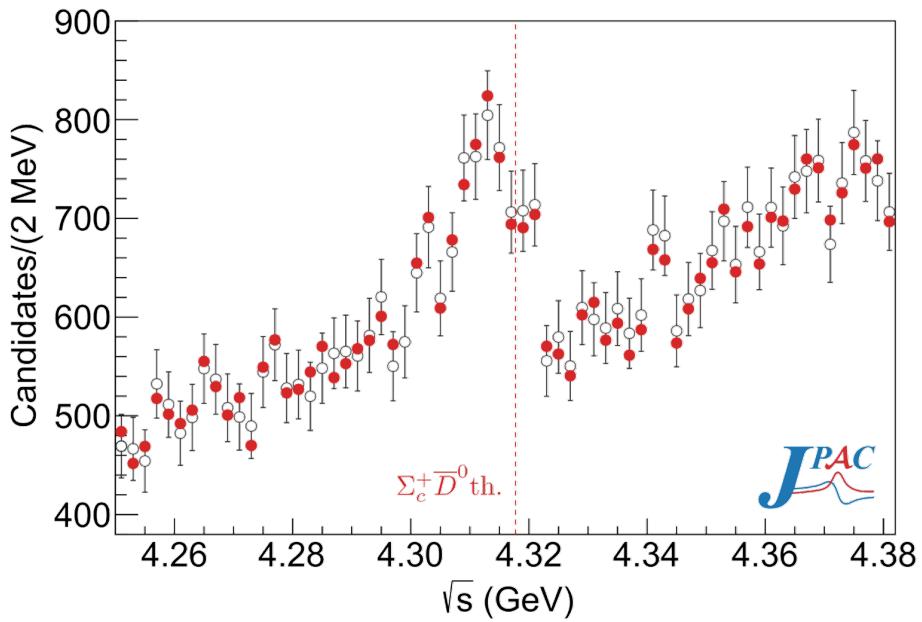

We generate compatible pseudodata from LHCb data.

We fit each of them with our amplitudes considering the experimental resolution.

Fit and error analysis

To fit the data and to estimate the sensitivity of the pole positions to the uncertainties, we use the bootstrap technique with 10^4 pseudodata sets.
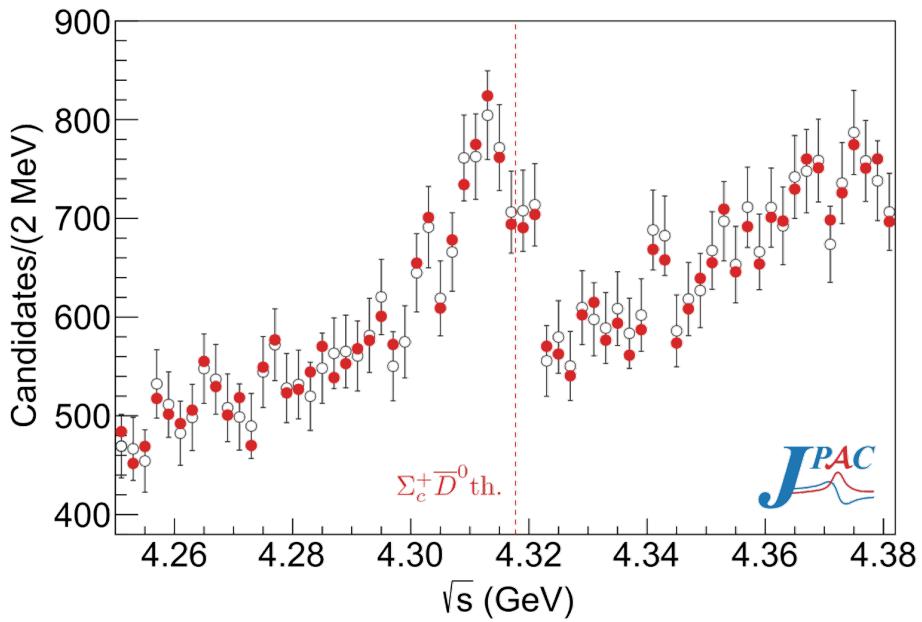

We generate compatible pseudodata from LHCb data.

We fit each of them with our amplitudes considering the experimental resolution.

We obtain the pole position onto the complex energy plane.

Fit and error analysis

To fit the data and to estimate the sensitivity of the pole positions to the uncertainties, we use the bootstrap technique with 10^4 pseudodata sets.
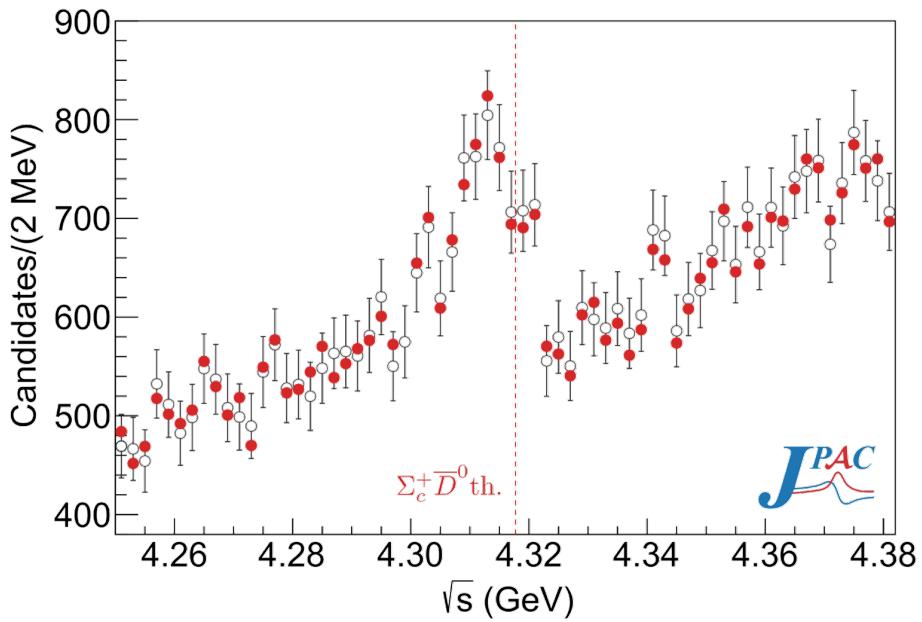

We generate compatible pseudodata from LHCb data.

We fit each of them with our amplitudes considering the experimental resolution.

We obtain the pole position onto the complex energy plane.

This technique allows to propagate the uncertainties from the data to the parameters and poles, accounting for the correlations.

Fit results – Scattering length
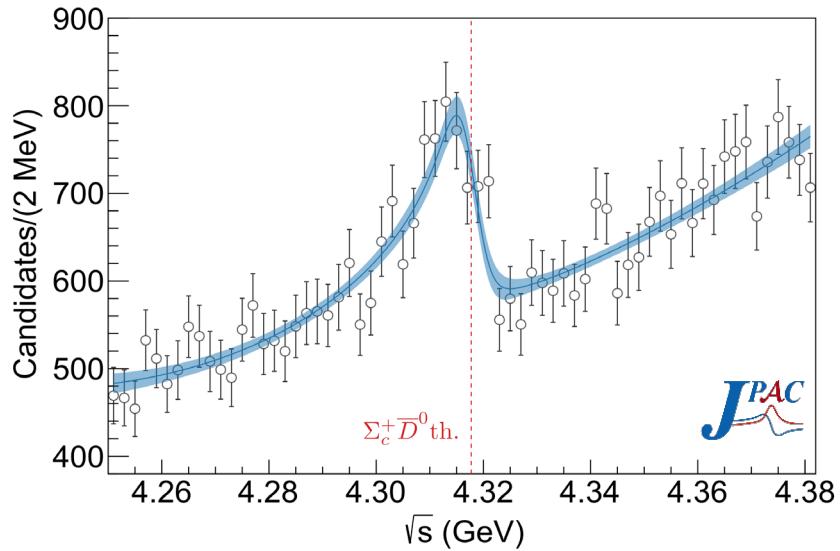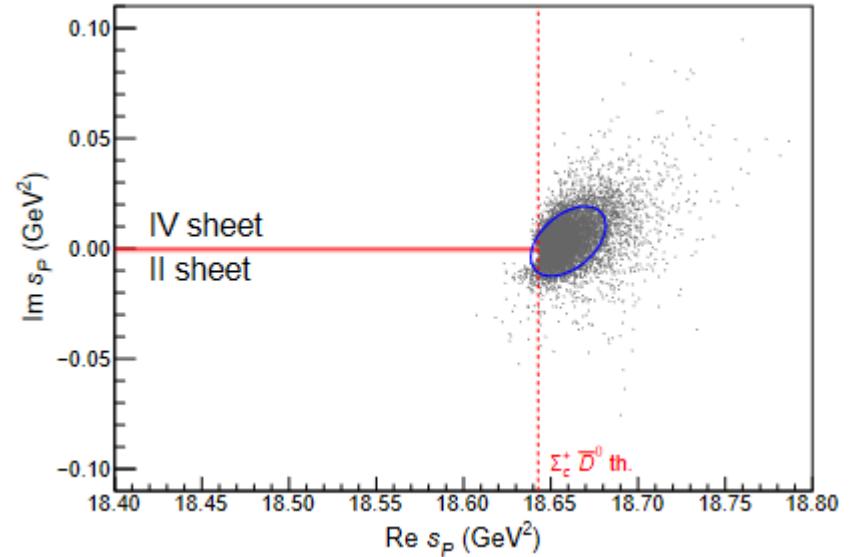
Fit to the $\cos\theta_{P_c}$-weighted $J/\psi\,p$ mass distribution from LHCb

Fit results – Scattering length
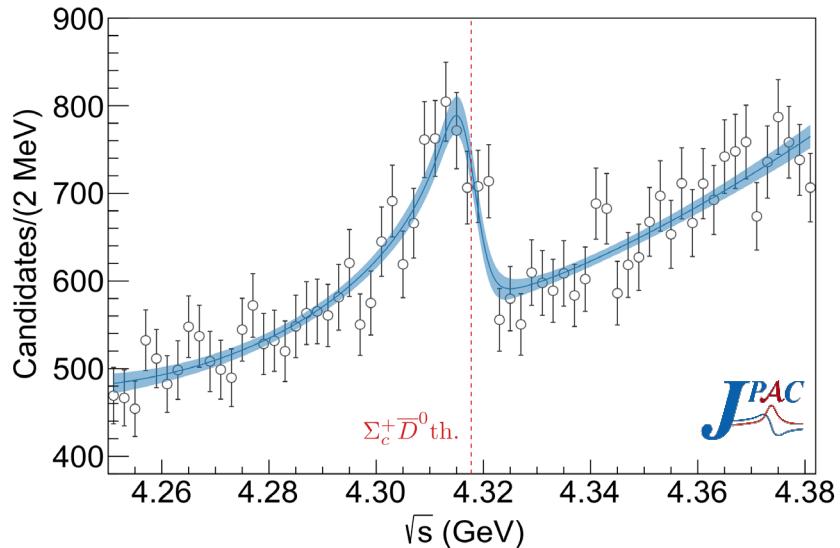
Fit to the $\cos\theta_{P_c}$-weighted $J/\psi\, p$ mass distribution from LHCb
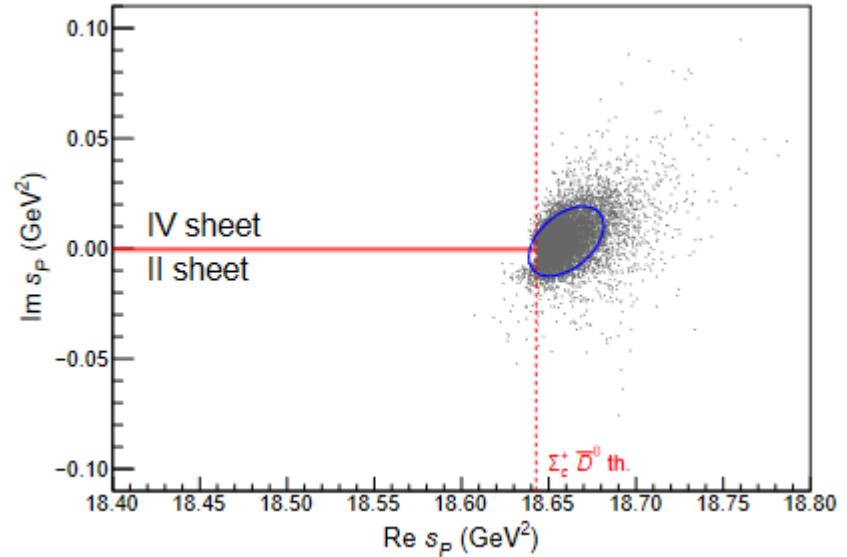
$$\chi^2/dof = 48.1/(66-7) = 0.82$$

Fit results – Scattering length
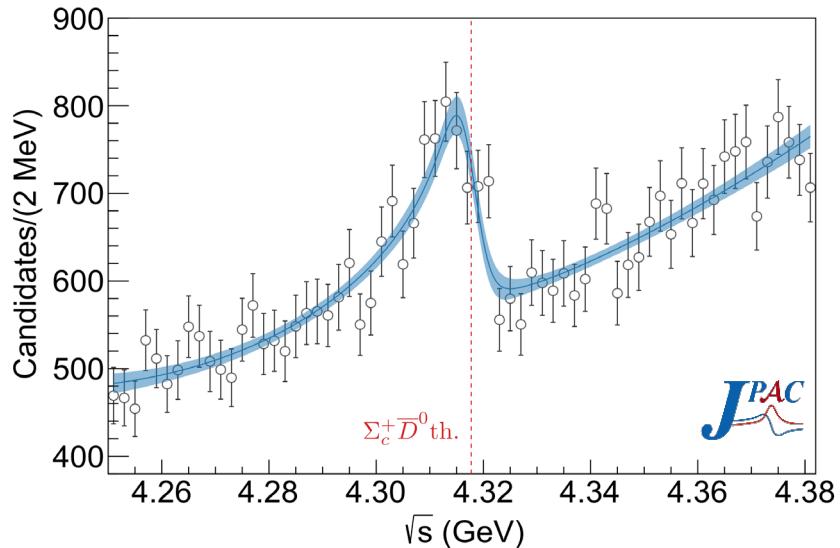
Fit to the $\cos \theta_{P_c}$-weighted $J/\psi\, p$ mass distribution from LHCb
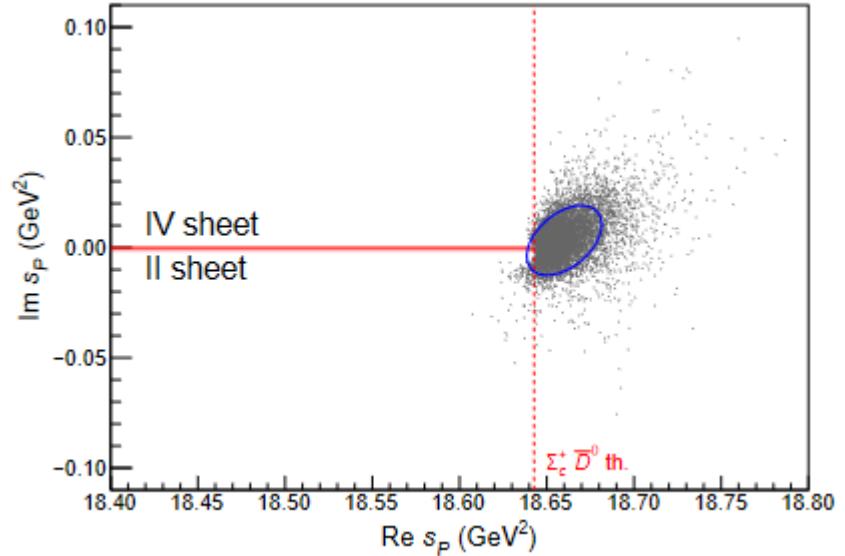
$$\chi^2/dof = 48.1/(66-7) = 0.82$$

Pole position

$M = 4319.7 \pm 1.6 \text{MeV}$

$\Gamma = -0.8 \pm 2.4 \text{MeV}$

Fit results – Effective range
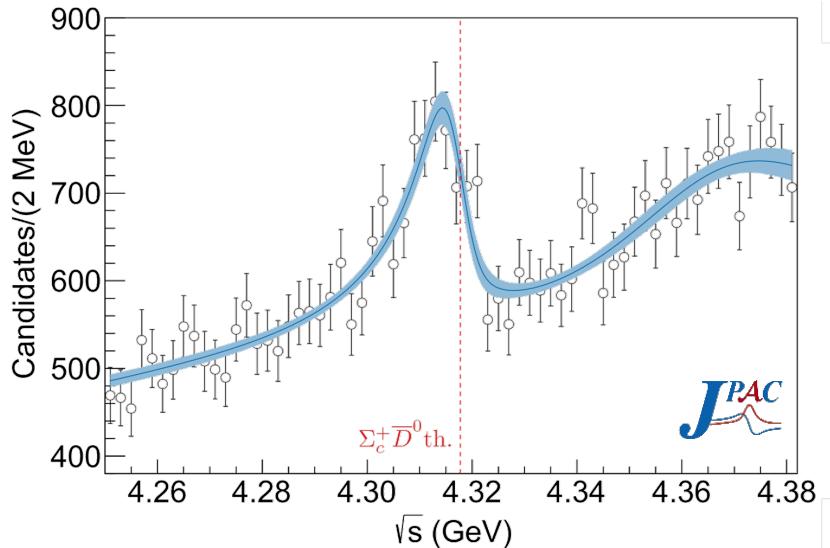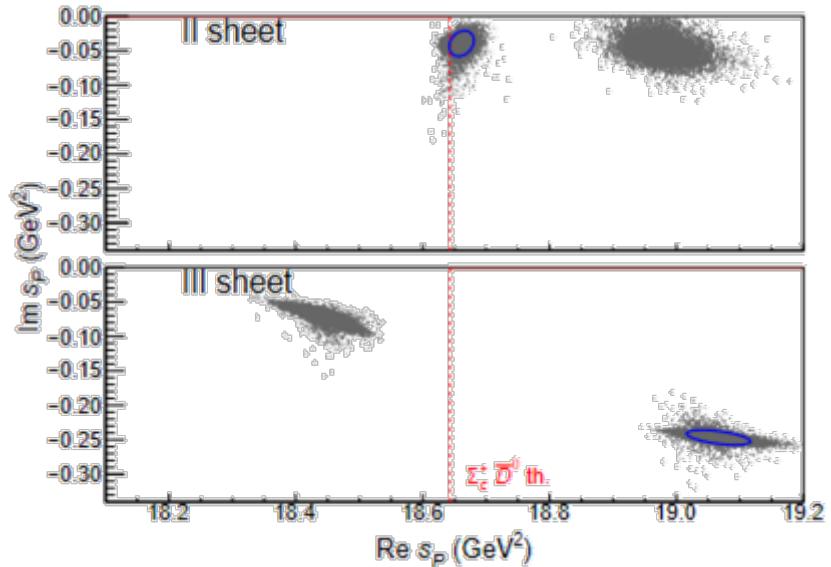
Fit to the $\cos\theta_{P_c}$-weighted $J/\psi\, p$ mass distribution from LHCb

Fit results – Effective range
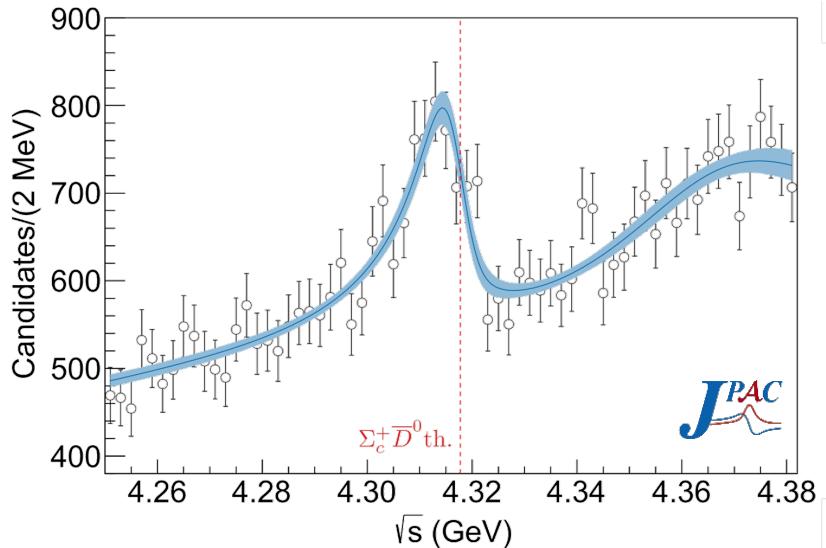
Fit to the $\cos \theta_{P_c}$-weighted $J/\psi\, p$ mass distribution from LHCb
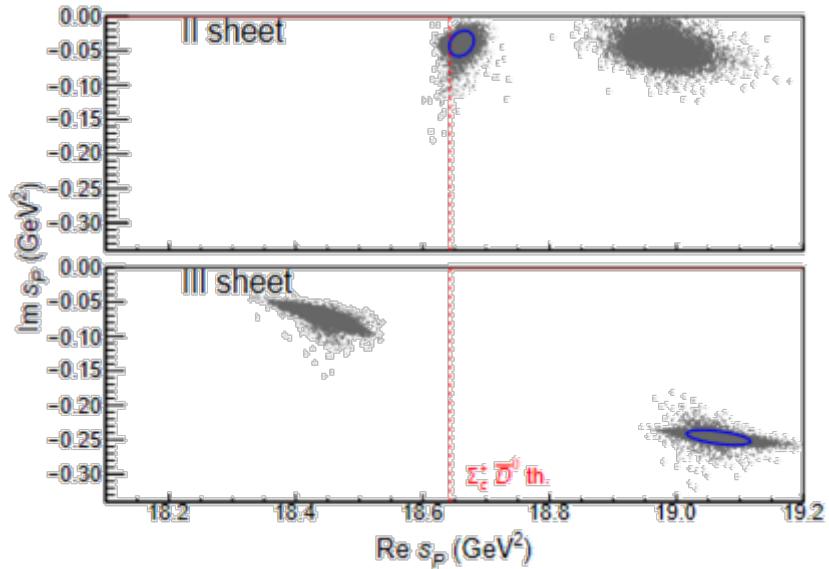
$$\chi^2/dof = 43/(66 - 9) = 0.75$$

Fit results – Effective range
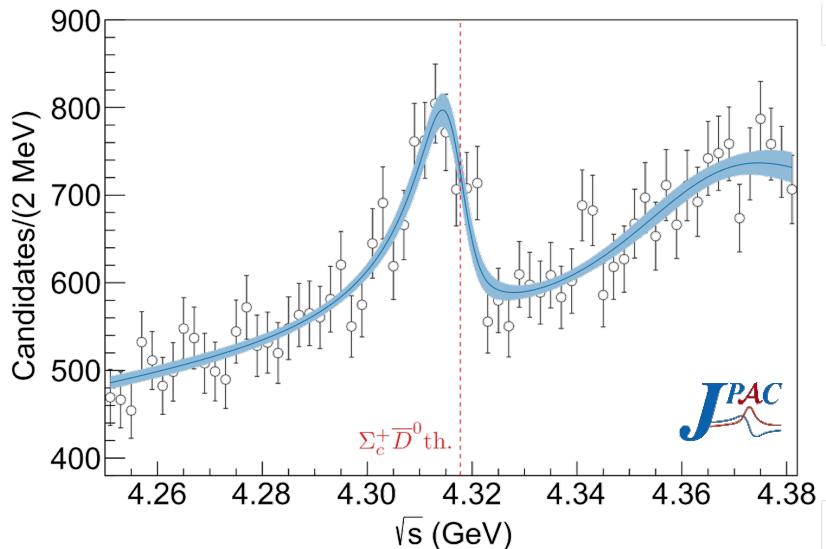
Fit to the $\cos \theta_{P_c}$-weighted $J/\psi\, p$ mass distribution from LHCb
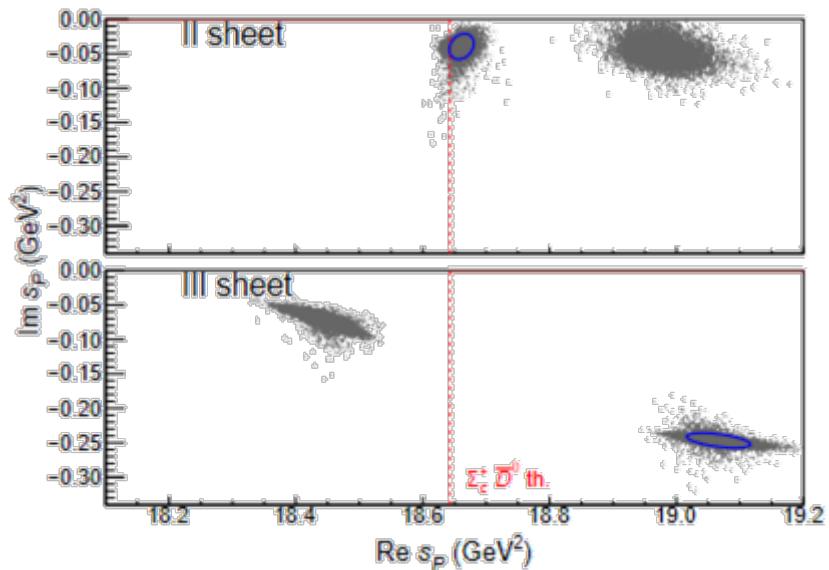
$$\chi^2/dof = 43/(66 - 9) = 0.75$$

Pole position

$$M = 4319.8 \pm 1.5\,\text{MeV}$$

$$\Gamma = 9.2 \pm 2.9\,\text{MeV}$$

Which model is better?

In both cases the pole position results are compatible with the threshold-driven signal hypothesis.

Which model is better?

In both cases the pole position results are compatible with the threshold-driven signal hypothesis.

The preference of effective range ($c_{ii} \neq 0$) over the scattering length ($c_{ii} = 0$) is only at 1.8σ level calculated with the Wilks theorem and we consider both cases as equally acceptable.

Which model is better?

In both cases the pole position results are compatible with the threshold-driven signal hypothesis.

The preference of effective range ($c_{ii} \neq 0$) over the scattering length ($c_{ii} = 0$) is only at 1.8σ level calculated with the Wilks theorem and we consider both cases as equally acceptable.

Further interpretation can be drawn by changing the amplitude parameters and studying the movement of singularities.

Channel decoupling and pole movement
Scattering length

We track down the movement of the poles as the coupling between the two channels is reduced. By taking $m_{12} \rightarrow 0$.

Channel decoupling and pole movement
Scattering length

We track down the movement of the poles as the coupling between the two channels is reduced. By taking $m_{12} \to 0$.
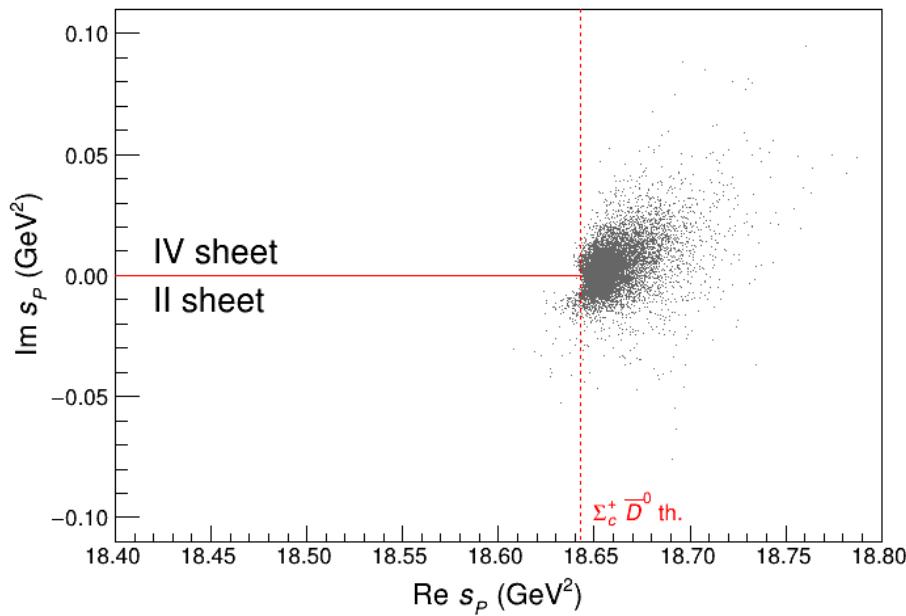
Channel decoupling and pole movement
Scattering length

We track down the movement of the poles as the coupling between the two channels is reduced. By taking $m_{12} \to 0$.

The fraction of poles that reach the real axis from the lower side of the II sheet is 0.7% only, and thus not significant. Meaning that the binding is insufficient to form a molecule.

Channel decoupling and pole movement
Scattering length

We track down the movement of the poles as the coupling between the two channels is reduced. By taking $m_{12} \to 0$.
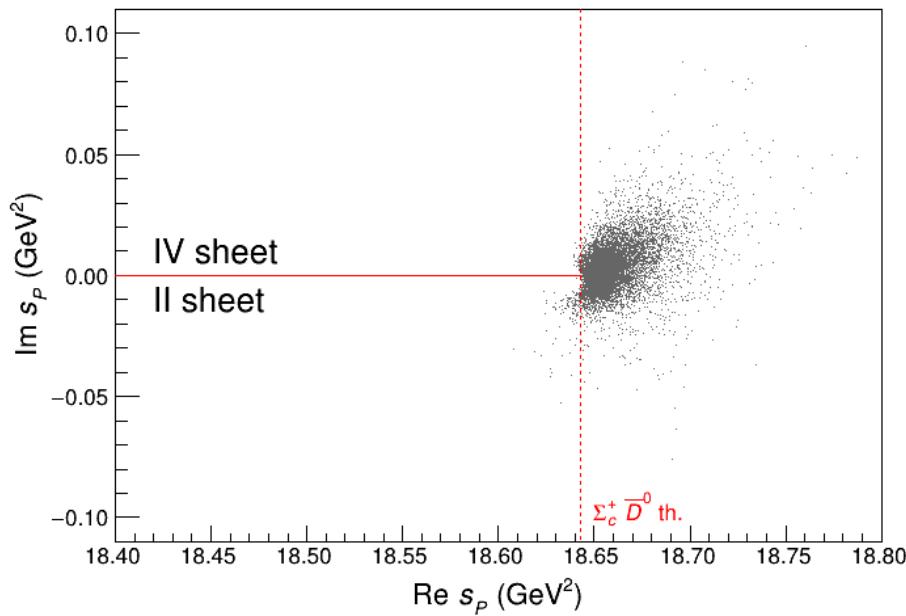

The fraction of poles that reach the real axis from the lower side of the II sheet is 0.7% only, and thus not significant. Meaning that the binding is insufficient to form a molecule.

This result hints to the interpretation of the pole as an unbound virtual state

Channel decoupling and pole movement Effective range

Similarly we track down the movement of the poles as $m_{12} \to 0$.

$$\frac{[m_{22} - c_{22}s - ik_2]}{[m_{22} - c_{22}s - ik_2][m_{11} - c_{11}s - ik_1] - m_{12}^2}$$

Channel decoupling and pole movement
Effective range

Similarly we track down the movement of the poles as $m_{12} \to 0$.

$$\frac{[m_{22} - c_{22}s - ik_2]}{[m_{22} - c_{22}s - ik_2][m_{11} - c_{11}s - ik_1] - m_{12}^2}$$

Channel decoupling and pole movement
Effective range
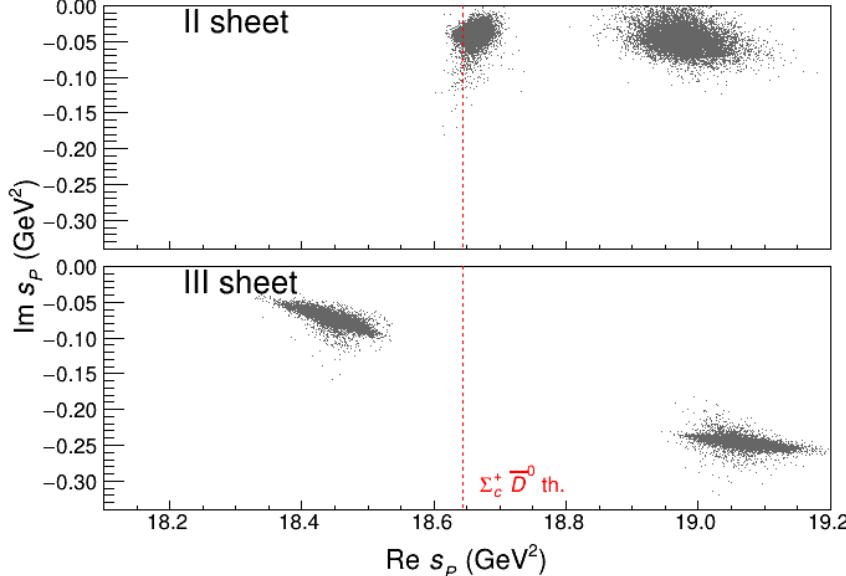
Similarly we track down the movement of the poles as $m_{12} \to 0$.

$$\frac{[m_{22} - c_{22}s - ik_2]}{[m_{22} - c_{22}s - ik_2][m_{11} - c_{11}s - ik_1] - m_{12}^2}$$

Channel decoupling and pole movement
Effective range

Similarly we track down the movement of the poles as $m_{12} \to 0$.

$$\frac{[m_{22} - c_{22}s - ik_2]}{[m_{22} - c_{22}s - ik_2][m_{11} - c_{11}s - ik_1] - m_{12}^2}$$

**The motion to the furthest unphysical sheet suggest a virtual state too.**

DNN analysis using effective range model

Since the effective range parametrization, depending on the parameters values and the pole position classifies the states as {b|2,b|4,v|2,v|4} we can build and train a Neural Network to analyze the Pc data.

$$(m_{11} - ik_1)(m_{22} - ik_2) - m_{12}^2 = 0 \qquad q = -ik_2$$

$$\eta_1 = Sign\left(\frac{m_{12}^2}{m_{22} + q} - m_{11}\right) \qquad \eta_2 = Sign(Re[q])$$

Bound when $m_{22} > 0$
Virtual when $m_{22} < 0$

I   sheet $(+, +)$ II   sheet $(-, +)$
III sheet $(-, -)$ IV sheet $(+, -)$
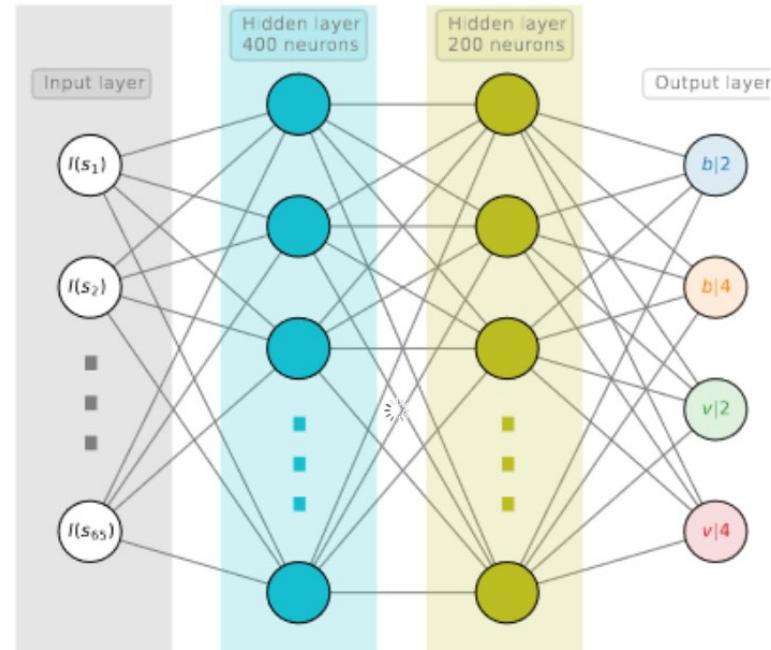
PhysRevD.105.L091501

DNN analysis using effective range model

The DNN consists of an input layer with as many nodes as there are energy bins, followed by two fully-connected hidden layers with 400 and 200 nodes respectively, and finally an output layer with four nodes that correspond to the four classes. After each hidden layer we set a dropout probability that randomly sets nodes to zero, to improve generalization performance. The DNN is trained using the Adam optimizer.
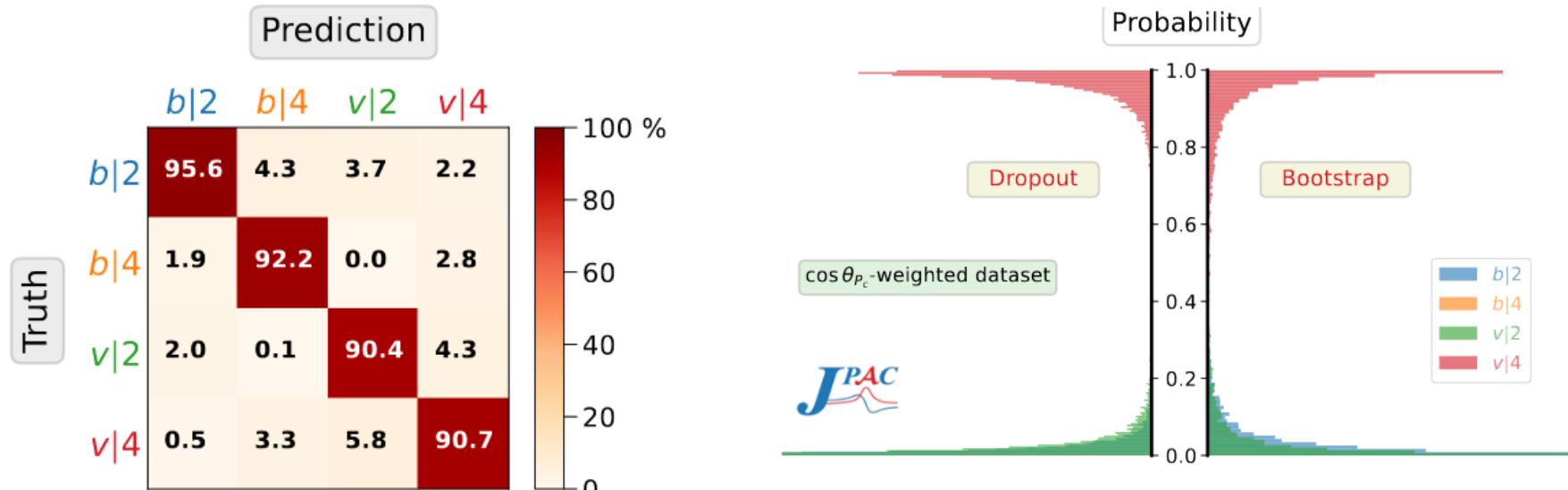
Confusion matrix for the case of $\sigma = 5\%$. Percentages refers to the prediction accuracy.

Dropout and Bootstrap classification probabilities densities for the predictions con $\cos(\theta_{P_c})$ −weighted LHCb dataset.

Conclusions

- We have studied the Pc(4312) reported by LHCb in the $J/\psi\, p$ spectrum considering a reaction amplitude which satisfices the general principles of the S-matrix theory with a minimum bias from the underlying theory.

- We fitted the mass spectrum in the 4312 MeV mass region including the experimental resolution.

- The statistical uncertainties in the data were propagated to the extracted poles using the Bootstrap (Monte Carlo) technique.

- We study the three datasets provided by LHCb obtaining consistent results.

- Based on a systematic analysis of the reaction amplitudes and the data we favor a threshold-generated state interpretation of Pc(4312). In particular a virtual (unbound) state interpretation.

More on: JPAC, PRL 123 (2019) 092001

PRD 105 (2022) L091501

Thank you for your attention

Questions?

Extra slides

Three channel case

We also performed a study of the three-channel case, including the $\Sigma_c^{++} D^-$ threshold
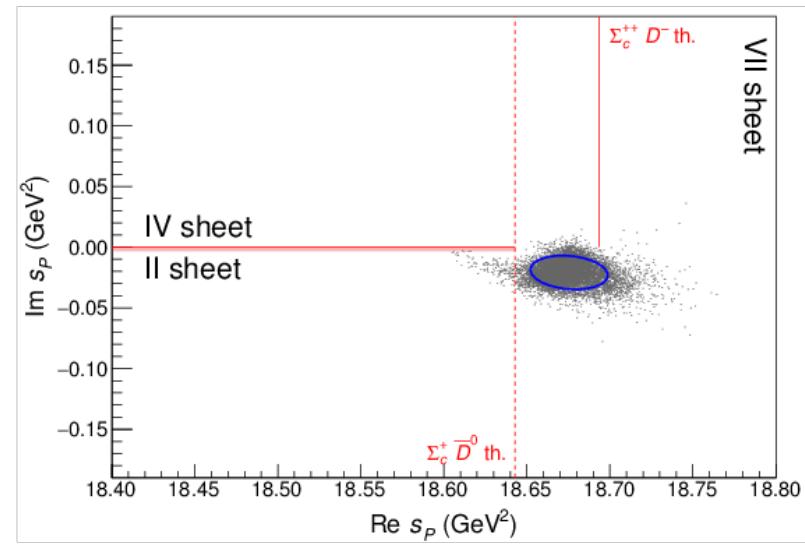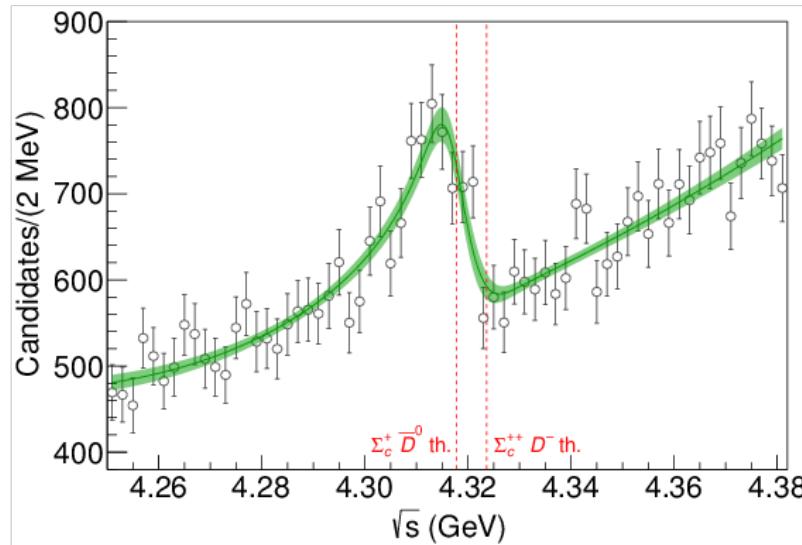
We find a single pole close to the $\Sigma_c^+ \overline{D}^0$ threshold on the II Riemann sheet.

K-matrix analysis

Using a single K-matrix pole with an off-diagonal constant background leads to a pole on the II sheet in the same position as case A ($c_{ij} = 0$).
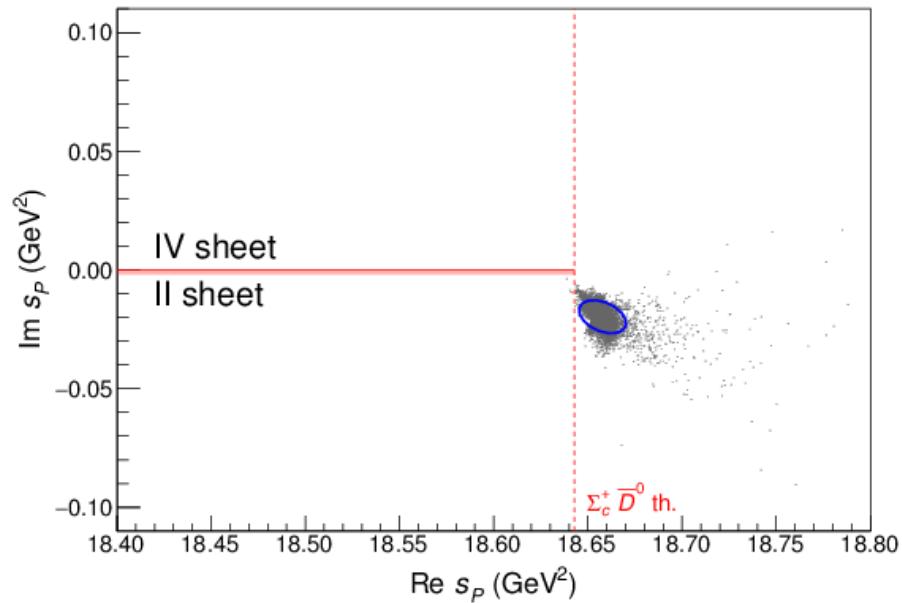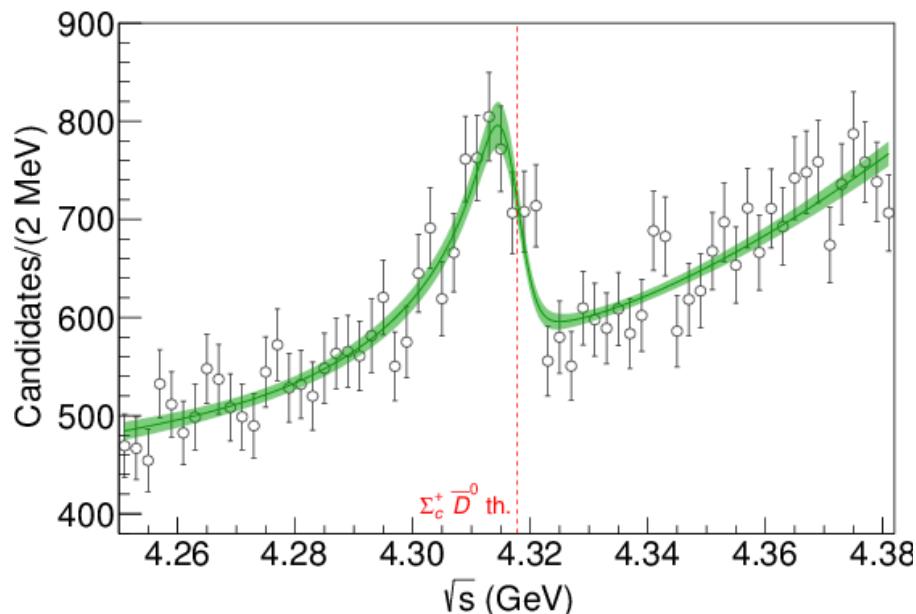
Flatté parametrization

The Flatté parametrization does not provide a good description of the $Pc(4312)^+$ peak, and does not generate stable poles in the region of interest.
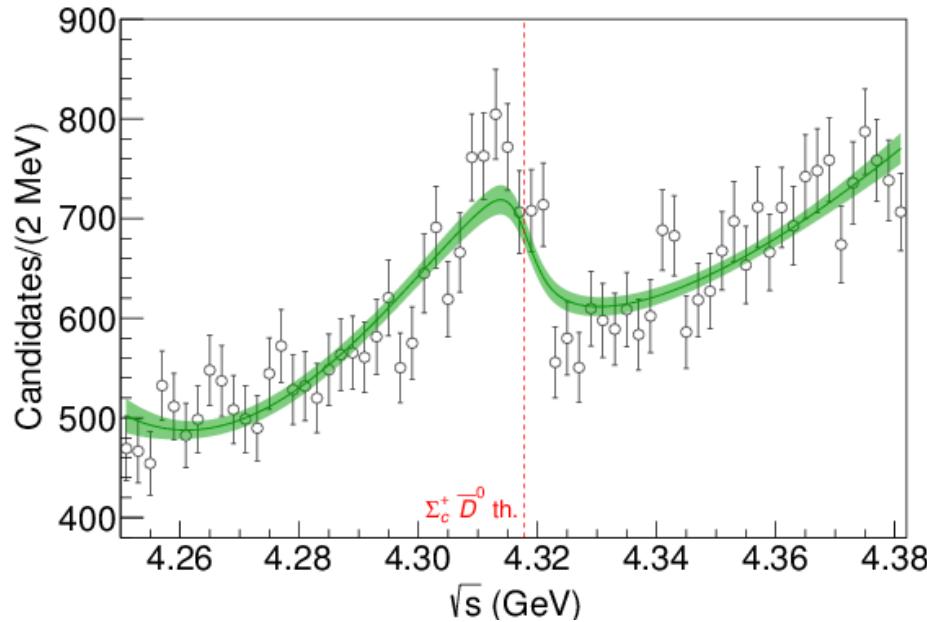
Three channel case – Pole movement

When the couplings between the channels are reduced, the pole quickly moves far to the left (on different sheets depending on the specific solution considered, as shown here), and cannot interpreted as a physical state.

See:
http://cgl.soic.indiana.edu/jpac/pc4312.php
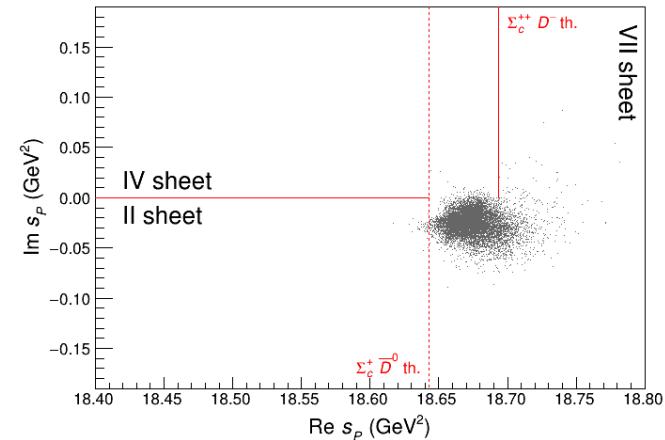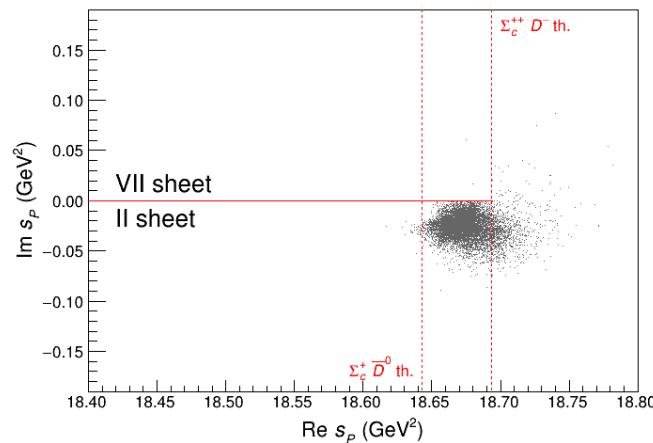
Fit results

$$T(s) = \begin{pmatrix} m_{11} - c_{11}s - i\sqrt{s - s_1} & m_{12} & \xi\, m_{12} \\ m_{12} & m_{22} - c_{22}s - i\sqrt{s - s_2} & \xi\, m_{23} \\ \xi\, m_{12} & \xi\, m_{23} & 1 + \xi\left(-1 + m_{22} - c_{22}s - i\sqrt{s - s_3}\right) \end{pmatrix}^{-1},$$

with $s_1 = (m_\psi + m_p)^2$, $s_2 = \left(m_{\Sigma_c^+} + m_{\bar{D}^0}\right)^2$, and $s_3 = \left(m_{\Sigma_c^{++}} + m_{D^-}\right)^2$. If $\xi = 0$ the amplitude $T(s)$ reduces to Eq. (2).

	Case A		Case B		3-channel	
χ^2/dof	$48.1/(66 - 7) = 0.82$		$43.0/(66 - 9) = 0.75$		$45.5/(66 - 8) = 0.78$	
	best fit	bootstrap	best fit	bootstrap	best fit	bootstrap
b_0	402.95	446 ± 73	0.74	6.1 ± 6.0	121.56	123.1 ± 1.4
b_1	-15.00	-17.4 ± 4.1	7.22	6.93 ± 0.36	0.63	0.52 ± 0.14
p_0	423.16	437 ± 16	85.06	92.6 ± 8.8	422.72	422.52 ± 0.38
p_1	-23.53	-24.28 ± 0.81	-5.30	-5.70 ± 0.47	-23.41	-23.409 ± 0.040
m_{11}	2.60	2.65 ± 0.28	151.29	151.35 ± 0.23	2.83	2.82 ± 0.19
m_{22}	0.22	0.223 ± 0.078	38.81	39.12 ± 0.28	-4.27	-4.259 ± 0.042
m_{12}	0.85	0.86 ± 0.11	1.03	1.035 ± 0.062	0.64	0.646 ± 0.057
m_{23}	0	0	0	0	4.38	4.385 ± 0.022
c_{11}	0	0	8.00	8.007 ± 0.015	0	0
c_{22}	0	0	2.06	2.081 ± 0.016	0	0
c_{12}	0	0	0	0	0	0
ξ	0	0	0	0	1	1

The off diagonal terms in our amplitude

In our analysis the off diagonal terms are:

$$P_2(s)T_{12} = P_2(s)\frac{m_{12}}{D(s)}$$

Where $D(s)$ is the denominator common to all T_{ij}'s and $P_2(s)$ is a smooth function.

It has the same singularity structure as T_{11} and its contribution can be absorbed into production parameters with no prejudice on the underlying theory.

Convoluting with resolution

The LHCb resolution which we name $R(E)$, where $E = \sqrt{s}$ is:

$$R(x) = 2.71 - 6.56 \times 10^{-6}(x - 4567)^2 \qquad \text{and } x \text{ in MeV}$$

The amplitude computed at energy E_0, convoluted with the resolution reads:

$$\frac{dN(E_0)}{d\sqrt{s}} = \frac{1}{A(E_0)} \int_{M_\psi + m_p}^{m_{\Lambda_b} - m_K} \frac{dN(E)}{dE} \exp\left[-\frac{(E_0 - E)^2}{2R^2(E_0)}\right] dE$$

And A is given by:

$$A(E_0) = \int_{M_\psi + m_p}^{m_{\Lambda_b} - m_K} \exp\left[-\frac{(E_0 - E)^2}{2R^2(E_0)}\right] dE$$

Riemann sheet structure
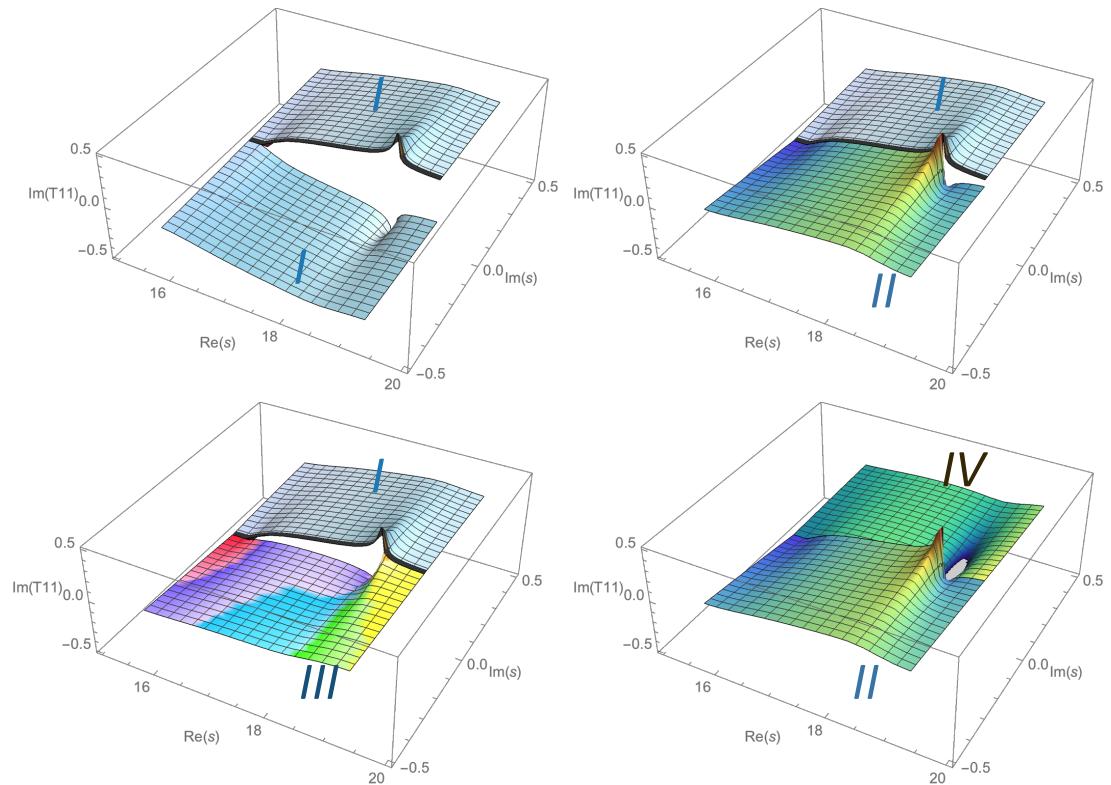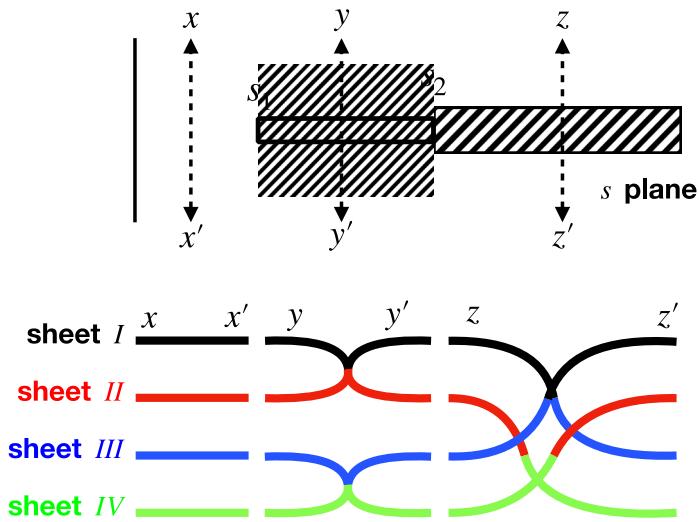
More detail on pole movement

$\Sigma_c^+ \overline{D}^0$

$J/\psi\ p$

$\Sigma_c^+ \overline{D}^0$

$J/\psi\ p$

$\Sigma_c^+ \overline{D}^0$

$J/\psi\ p$

More detail on pole movement

$\Sigma_c^+ \overline{D}^0$

$J/\psi\ p$

$\Sigma_c^+ \overline{D}^0$

$J/\psi\ p$

$\Sigma_c^+ \overline{D}^0$

$J/\psi\ p$

More detail on pole movement

$\Sigma_c^+ \overline{D}^0$

$J/\psi\ p$

2 sheet

3 sheet

$\Sigma_c^+ \overline{D}^0$

$J/\psi\ p$

2 sheet

$\Sigma_c^+ \overline{D}^0$

4 sheet

$J/\psi\ p$
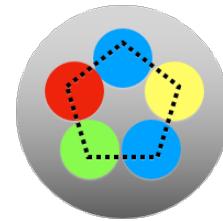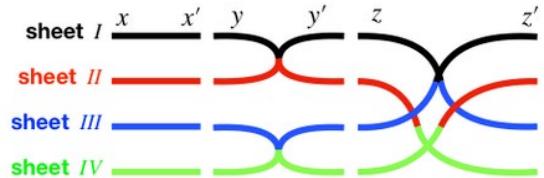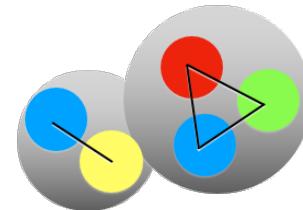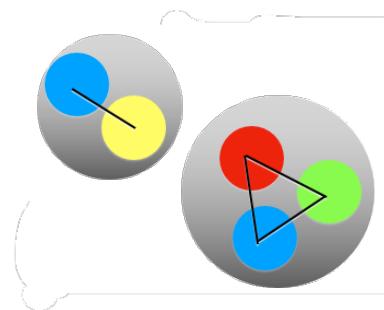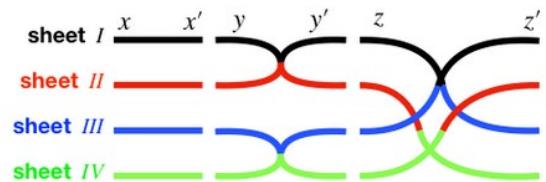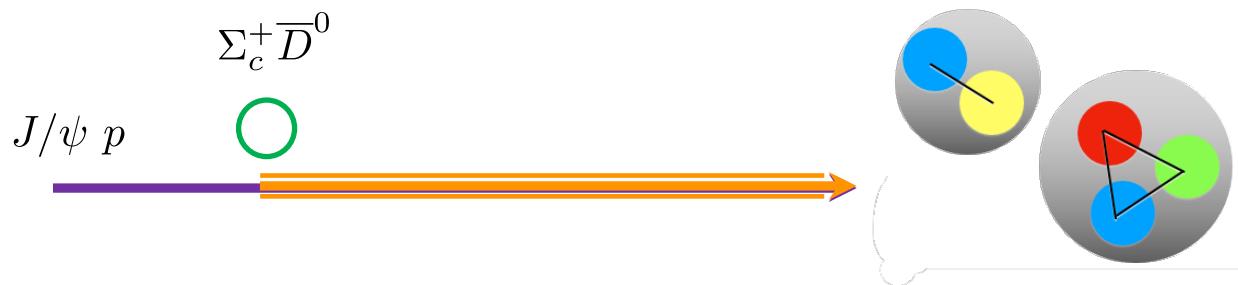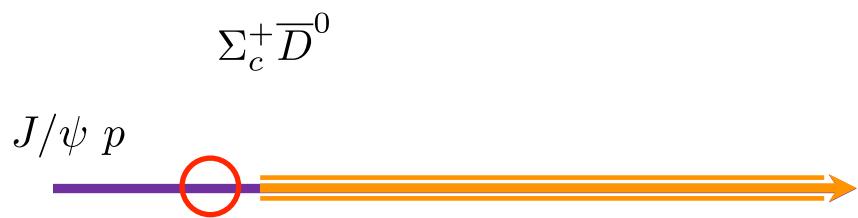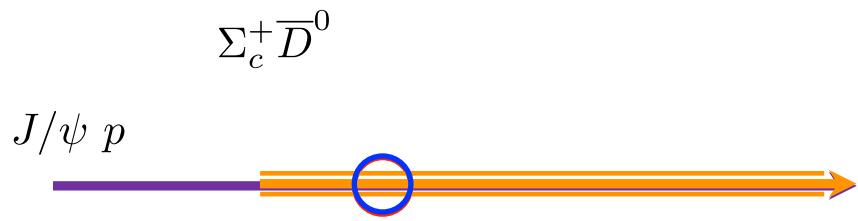
2 sheet
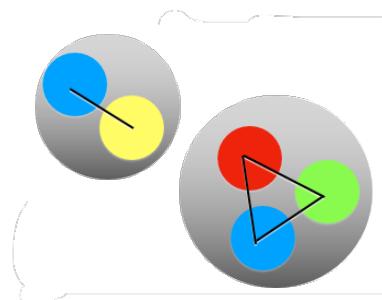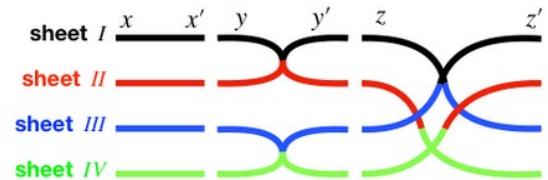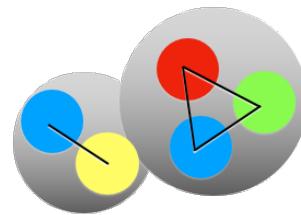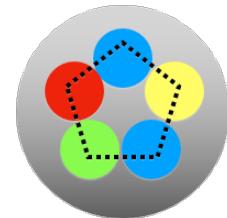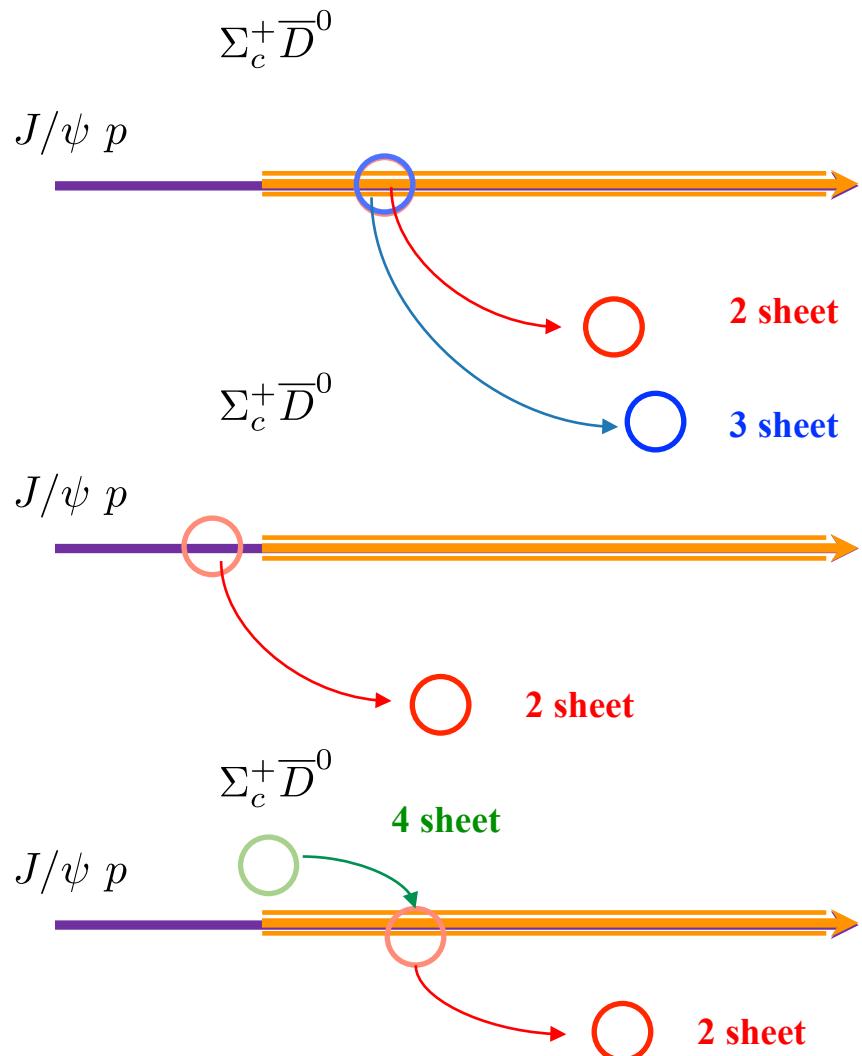
LHCb really affirmed that the state is a molecule?

The minimal quark content of these states is $duuc\bar{c}$. Since all three states are narrow and below the $\Sigma_c^+ \bar{D}^0$ and $\Sigma_c^+ \bar{D}^{*0}$ ($[duc][u\bar{c}]$) thresholds within plausible hadron-hadron binding energies, they provide the strongest experimental evidence to date for the existence of bound states of a baryon and a meson. The $\Sigma_c^+ \bar{D}^0$ ($\Sigma_c^+ \bar{D}^{*0}$) threshold is within the extent of the $P_c(4312)^+$ [$P_c(4457)^+$] peak, and therefore virtual [38] rather than bound states are among the plausible explanations. In simple tightly bound pentaquark models, the proximity of these states to baryon-meson thresholds would be coincidental, and furthermore, it is difficult to accommodate their narrow widths [39]. A potential barrier between diquarks, which could separate the c and $\bar{c}$ quarks, has been proposed to solve similar difficulties for tetraquark candidates [40]. An interplay between tightly bound pentaquarks and the $\Sigma_c \bar{D}$, $\Sigma_c \bar{D}^*$ thresholds may also be responsible for the P_c^+ peaks [41–44]. Therefore, such alternative explanations cannot be ruled out. Proper identification of the internal structure of the observed states will require more experimental and theoretical scrutiny.

It is necessary to do a much more detailed study to determine the nature of this signal

We need more information about the quantum numbers of this state

This could be the first virtual state found in nature and could open the window to study a new physics

S-matrix theory

Operator whose elements quantify the transition between an initial $|a\rangle$ to a final $|b\rangle$ state.

$$S(s,t) = I + 2iT(s,t)$$

- ○ *Something happens*   Unitarity
- ○ *Causality*   Analyticity
- ○ *Particle-Antiparticle*   Crossing symmetry

+Additional symmetries v.g. gauge, quiral, …

The scattering amplitude is an analytic function in the complex plane

s-channel u-channel

t-channel   decay channel